ARTICLE

Facile Synthesis of PbS Truncated Octahedron Crystals with High Symmetry and Their Large-Scale Assembly into Regular Patterns by a Simple Solution Route

Ning Wang,[†] Xia Cao,[†] Lin Guo,[†,‡,*] Shihe Yang,[‡,*] and Ziyu Wu[§,*]

[†]School of Materials Science and Engineering, Beijing University of Aeronautics and Astronautics, Beijing, 100083, China, , [‡]Department of Chemistry, The Hong Kong University of Science and Technology, Clear Water Bay, Kowloon, Hong Kong, China, and [§]Institute of High Energy Physics, Chinese Academy of Science, Beijing 100039, China

ABSTRACT Highly regular patterns with amazingly well-defined uniform truncated octahedrons of PbS nanocrystals as building blocks were prepared *via* a simple one-pot solution method. Each truncated octahedron has a composition of six {100} squares and eight {111} hexagons, and the overall structure shares 24 identical edges in a mecon way. Hexapod PbS, six-arm star-shaped dendrites, octahedron and truncated cubes were also fabricated. Structural and optical properties as well as morphological evolutions were studied by transmission electron microscopy, scanning electron microscopy, X-ray diffraction, and a confocal Raman spectroscopy. A mechanism for the formation of the PbS nanocrystals as well as their inner structure was tentatively proposed based on the characterization results.

KEYWORDS: PbS · truncated octahedron · self-assembly · Raman

Nanostructured materials are receiving increasingly interest in recent years due to their unique physical and chemical properties and potential applications in nanoscale devices.[1]

As a semiconductor compound, PbS is an important $\pi-\pi$ semiconductor material with a narrow band gap energy and large exciton Bohr radius (18 nm).[2] Moreover, quantum-size PbS has exceptional third-order nonlinear optical properties, which means it should be useful for optical devices such as optical switches.[3] Different morphologies of PbS nanocrystals have been achieved by various methods. For example, cubic-shaped PbS micro- and nanocrystals have been produced by the decomposition of a single-source precursor and a solution reflux method.[4,5] Rodlike PbS nanocrystals have been obtained using a combination of surfactant and polymer matrix as a template.[6] PbS nanowires as well as nanosheets have been prepared by a polymer-assisted solvothermal method.[7,8] Rod-based PbS multipods were synthesized from the thermal decomposition of a molecular precursor.[9] Star-shaped PbS microcrystals with eight symmetric arms along the ⟨111⟩ direction have been formed by an aqueous phase route.[4,10,11] Besides this, dendrites have recently attracted much attention due to the interesting morphology, properties, and potential applications as one type of attractive supramolecular structure.[12,13]

Self-assembly (SA) is the autonomous organization of components into patterns or structures without human intervention and now is popular for providing a simple, versatile method to prepare a modified surface at a high-level of order.[14,15]

A variety of natural systems with self-assembly properties has been used for this purpose, including lyotropic liquid crystals,[16] anodized alumina membranes,[17] block copolymers,[18] and close packed arrays of polystyrene latex and silica spheres.[19,20] The good homogeneity and organization, together with better controlling the microenvironment of the recognition molecules, make SA attractive in bimolecular electronics and biosensor development.[21]

Excellent studies on the self-assembly of various novel colloidal nanocrystals have been carried out, and great achievements have been made.[9,10] However, to the best of our knowledge, little work has been focused on the self-assembly of PbS nanostructures with a highly geometrical shape, no report has been yet focused on how they are assembled, and the architectural control of PbS nanobuilding blocks with well-

*Address correspondence to guolin@buaa.edu.cn, chsyang@ust.hk, wuzy@ihep.ac.cn.

Received for review July 4, 2007 and accepted January 07, 2008.

Published online January 19, 2008. 10.1021/nn7000855 CCC: $40.75

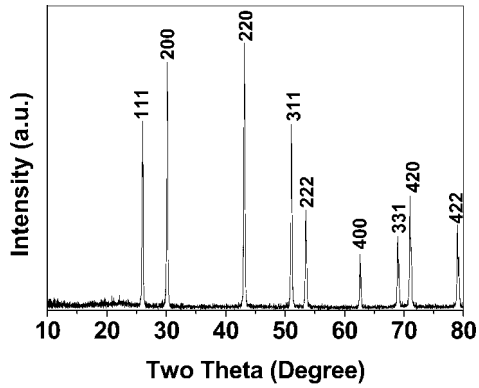

Figure 1. X-ray diffraction pattern of the as-prepared PbS samples.

defined shapes and arrays remains a key obstacle to overcome in the discovery of novel nanoscale properties and is essential for the success of "bottom-up" approaches toward future nanodevices.[1,22–24]

Hence, in this paper, we report on the one-step synthesis of high-quality PbS truncated octahedrons and their *in situ* large-scale self-assembly into sievelike patterns using a mild solution method without any post-treatment. This makes the free spatial arrangement possible. The novelty of this work is characterized by a one-pot procedure which combines formation of nanoparticle precursor, morphology evolution, three-dimensional (3D) assembly, and pattern shaping under easily controlled mild conditions. In addition, the unique optical properties of these novel nanopatterns are also reported.

RESULTS AND DISCUSSIONS

Figure 1 is the X-ray diffraction (XRD) pattern of the as-prepared sample that shows a high degree of crystallinity. All of the peaks match well with Bragg reflections of the standard face-center cubic (fcc) structure of PbS (space group: *Fm*3*m* (225), $a = 0.5936$ nm, JCPDF # 05-0592). It is worth noting that the ratio between the intensities of the (200) and (111) diffraction peaks is somewhat higher than the conventional value (1.30 *vs* 1.19), which indicates that our products may be abundant in {100} facets, and thus lead to relatively greater accelerated growth along the ⟨100⟩ directions.

The morphology of the PbS patterns built by truncated octahedron crystals with highly geometrical symmetry was visualized by scanning electron microscopy (SEM) and transmission electron microscopy (TEM). Typical SEM and TEM images of Figure 2 clearly show that the building block possesses a simple and amazingly well-defined uniform truncated octahedron structure with 14 faces. Each truncated octahedron has a composition of six squares and eight hexagons, and the overall structure shares 24 identical edges in a mecon way (Figure 2A). It is appealing that a synthetic technique as simple as the one presented here can produce such beautiful objects.

Detailed information about the nanopattern such as size and crystallinity of the building blocks can also be revealed by close examination. The SEM and TEM characterizations (Figures 2A−D) exhibit uniform PbS truncated octahedron crystals with average diameter of 180 nm and a strong preference for self-assembly of these truncated octahedron crystals into separate close-packed patterns by sharing their square faces. High-resolution TEM images (Figure 2, panels C and D) and the sharp Fourier transform pattern (Figure 2D inset), which can be obtained from any nanoparticle within the nanopatterns, reveals well-resolved lattice fringes corresponding to (200) planes of the PbS nanoparticles within the nanopattern, confirming well crystallinity for the nanoparticles and thus assembled nanopatterns. Meanwhile, no other minor shapes are observed around the edges of the assembly of these truncated particles, which suggests a growth mechanism of Ostwald ripening.

Raman spectra of the samples were collected using confocal Raman spectroscopy. The sample deposited on a quartz glass substrate was globally illuminated by a helium−neon (He−Ne) laser operating at 632.8 nm. The signal integration time was 50 s. In our experiments, the maximal laser power delivered to the sample was 15 mW and could be monitored *via* a filter wheel with optical densities of 0.3, 1, and 2, which were abbreviated as D0.3, D1, and D2, respectively. A typical Raman spectrum of the PbS crystals with 50 mW laser power is shown in Figure 3 (monitored by D2, which means the laser power delivered to the sample after monitored by D2 was 0.15 mW, but only about 50 μW reached the sample surface). According to earlier reports,[25,26] for the PbS materials, Raman peaks at 210, 271, and 451 cm^{-1} should be observed, corresponding to a 1 longitudinal optical phonon mode, a two-phonon process, and a 2 longitudinal optical phonon mode, respectively. It is well-known that in a crystalline semiconductor the observed Raman shifts usually correspond to the longitudinal optical phonons (LO), whereas other modes, such as the transverse optical phonons (TO) and the surface phonons (SP), are, in general, not observable because of symmetry restrictions and low intensities, respectively. However, as the surface-to-volume ratio is large for nanostructured materials, it is possible to observe the SP mode by Raman scattering measurements. In our experiment, the peak at 190 cm^{-1} should be identified to be due to the SP mode, and its intensity increases greatly with the decreasing crystal size, and the SP mode is so intense that the peaks at 210 and 271 cm^{-1} become two small shoulders and are difficult to characterize.

From Batonneau's work,[27] a peak at 966 cm^{-1} will appear due to the photodegradation of PbS when the laser power was increased to 15 mW. It should be a characteristic peak for the oxidation products $PbSO_4$, PbO−$PbSO_4$, 3PbO−$PbSO_4$, and 4PbO−$PbSO_4$. So, ad-

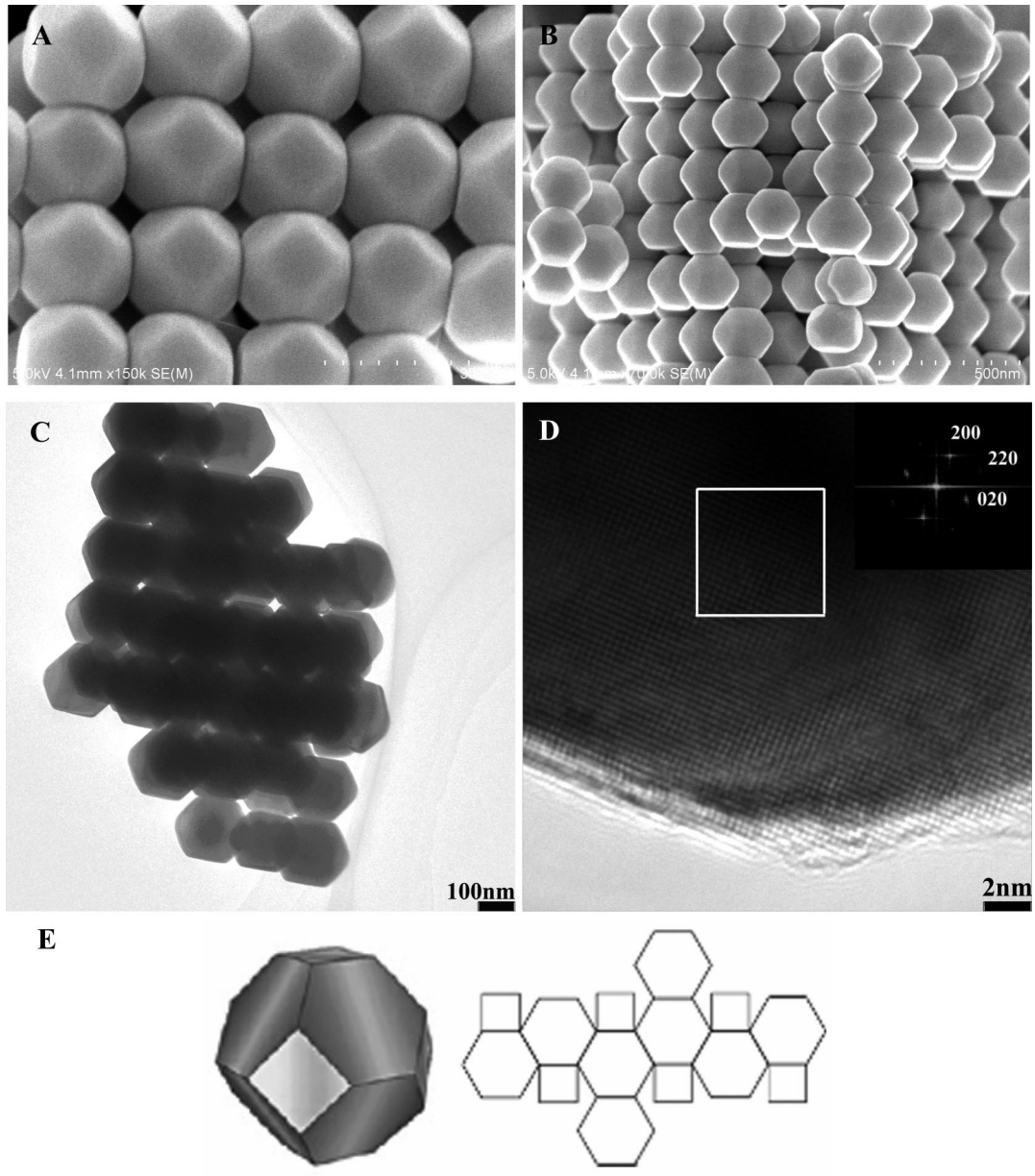

Figure 2. (A and B) FESEM images of the as-prepared PbS nanopatterns. (C and D) High-resolutions TEM images of the PbS nanopatterns. (E) Schematic illustration of a truncated octahedron with 14 faces (six squares and eight hexagons), composing the structure by sharing the identical 24 edges in a mecon way. Inset of panel D is the Fourier transform of the image. The scale bars of panels A, B, C, and D are 300, 500, 100, and 2 nm, respectively.

ditional Raman spectra were measured by other higher laser powers to test the photodegradation activity of our product, and the spectra of the sample with higher laser powers are shown in Figure 4. This result is surprising that when the laser power was increased to 0.5 mW (monitored by a filter D1, which means the laser power delivered to the sample was 1.5 mW, but only 0.5 mW reached the sample), the peak at 966 cm^{-1} was clearly observed (Figure 4a), and when the laser power was increased to 5 mW finally, the peaks at 431, 602, and 966 cm^{-1} were also observed (Figure 4c), which fit well with the result reported by Batonneau,[27] indicting that our product is sensitive to the laser and can be photodegraded at much lower laser power thus conve-

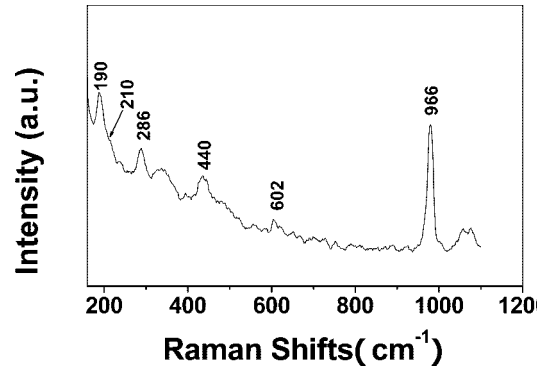

Figure 3. Raman spectra of the as-prepared PbS nanopattern samples.

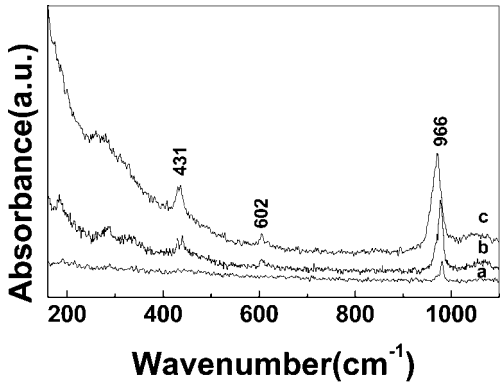

Figure 4. Raman spectra of PbS nanopatterns of truncated octahedrons with different laser powers: a, 0.5 mW (monitored by filter D1); b, 2.16 mW (monitored by filter D0.3); c, 5 mW (no filter, which means the laser power delivered to the sample was 15 mW but only 5 mW reached the sample).

niently converted to other environmental friendly materials. This may be caused by the shape and surface properties of the PbS crystals.

The growth mechanisms of PbS crystals have been well investigated in several papers. It has been shown that such novel morphologies such as dendritic[28–31] and star-shaped[9] structures occur through preferential growth of the truncated octahedron-shaped PbS seed ⟨100⟩ directions. In such a case, the presence of surfactant must be taken into consideration, for it has been reported that only star-shaped PbS crystals with eight ⟨111⟩-oriented arms are produced in the absence of surfactants under similar conditions.[33] Besides this, it is well-known that surface energies associated with different crystallographic planes are usually different and a general sequence can be elucidated as $\gamma\{111\} < \gamma\{100\} < \gamma\{110\}$.[32] Capping molecules such as CTAB can selectively stabilize the {111} faces, containing Pb or S only, since their ionic head groups can strongly interact with the charged {111} faces rather than the uncharged {100} faces, which contain mixed Pb/S. Thus the interaction between Pb and $-N(CH_3)_3^+$ ions can significantly elevate the activation energy of the {111} faces, leading to relatively greater accelerated growth on the {100} faces relative to the {111} faces. Furthermore, the shape of such an fcc nanocrystal as PbS is mainly determined by the ratio (R) between the growth rates along the {100} and {111} directions.[32] In our case, thiourea is a somewhat weak sulfur source. Higher concentrations surely can promote its reaction rate with Pb ions of different positions and gradually thus change the rate ratio. As a result, both the stable PbS nano- and microstructures such as six-arm star-shaped dendrites (Figure 5D) and the metastable nanostructures such as star-shaped multipods nanocrystals (Figures 5E, F) and octahedrons or truncated octahedrons (Figure 2) can be obtained. Still more interesting, the metastable nanostructure of a truncated octahedron tended to assemble into an orderly pattern as if to increase the portion of lower-index planes.

As reported,[32] an octahedron bounded by the most stable {111} planes will be formed when $R > 1.73$ (Figure 5A), and perfect cubes bounded by the less stable {100} planes will result if R is reduced to 0.58. The particles with $0.87 < R < 1.73$ have the {100} and {111} facets, which are named the truncated octahedral (TO) (Figure 2). The difference between the enhanced growth rates on the {100} and {111} planes induced the ratio R to have a value of more than 1.73, which resulted in the formation of the star-shaped dendrites as shown in Figure 5, panels C and D. Thus it can be deduced that as an integrated result of the capping effects of CTAB, the presence of both CTAB and thiourea with different molar ratios results in the formation of octahedrons with eight {111} faces and then intermediate morphology of truncated octahedron/mecon with 14 faces (six {100} squares and eight {111} hexagons) as well as the hexapods with six {100} arms. Therefore, CTAB plays the role of capping agent in the nucleation and growth of PbS crystals and the critical factor determining architectural features of the PbS nanocrystals. In other words, we can control the PbS shape evolution by simply tuning the molar ratio of the precursors and the surfactants while maintaining a fixed reaction time.

The formation of nanopatterns with such a regular symmetry may also be related to the oligomerization of lead acetate, a process that has been well discussed in many publications for the same or similar metal alkoxides.[33–35] That is, in the initial stage of refluxing, as refluxing was continued, through the formation of Pb−O− covalent and Pb←OH coordination bonds, the lead acetates tended to form longer chains, which could further self-assemble into ordered bundles (nanochains) through van der Waals interaction, where the metal salt generally remained as Pb(II) in the precursor nanopatterns. But in our case, 3D chaining of PbS nanocrystals with their highly symmetric cubic lattice is rather counterintuitive; the sizes of the single crystalline building blocks are in the region of hundreds of nanometers, which well pass the size limitation of precursor nanopatterns. Thus other more convincing mechanism should be introduced.

In other works,[36–40] Weller, Tang, Kotov, and Giersig identified the inherent anisotropy of crystal structure or crystal surface reactivity as the driving force for the particle assembly. For nanoparticles such as octahedron and truncated octahedron (Figure 2A), the surfaces of which are {111} and {100}, and the side edges of the octahedron are ⟨110⟩. The principles for assembling the NCs are to face the same type of faces, such as {111} to {111}, and align them in the same orientation to enhance the packing density,[41,42] resulting in a single-crystal structure of the entire array. This is driven by minimizing the interface mismatch energy by forming a coherent interface and reducing the exposed sur-

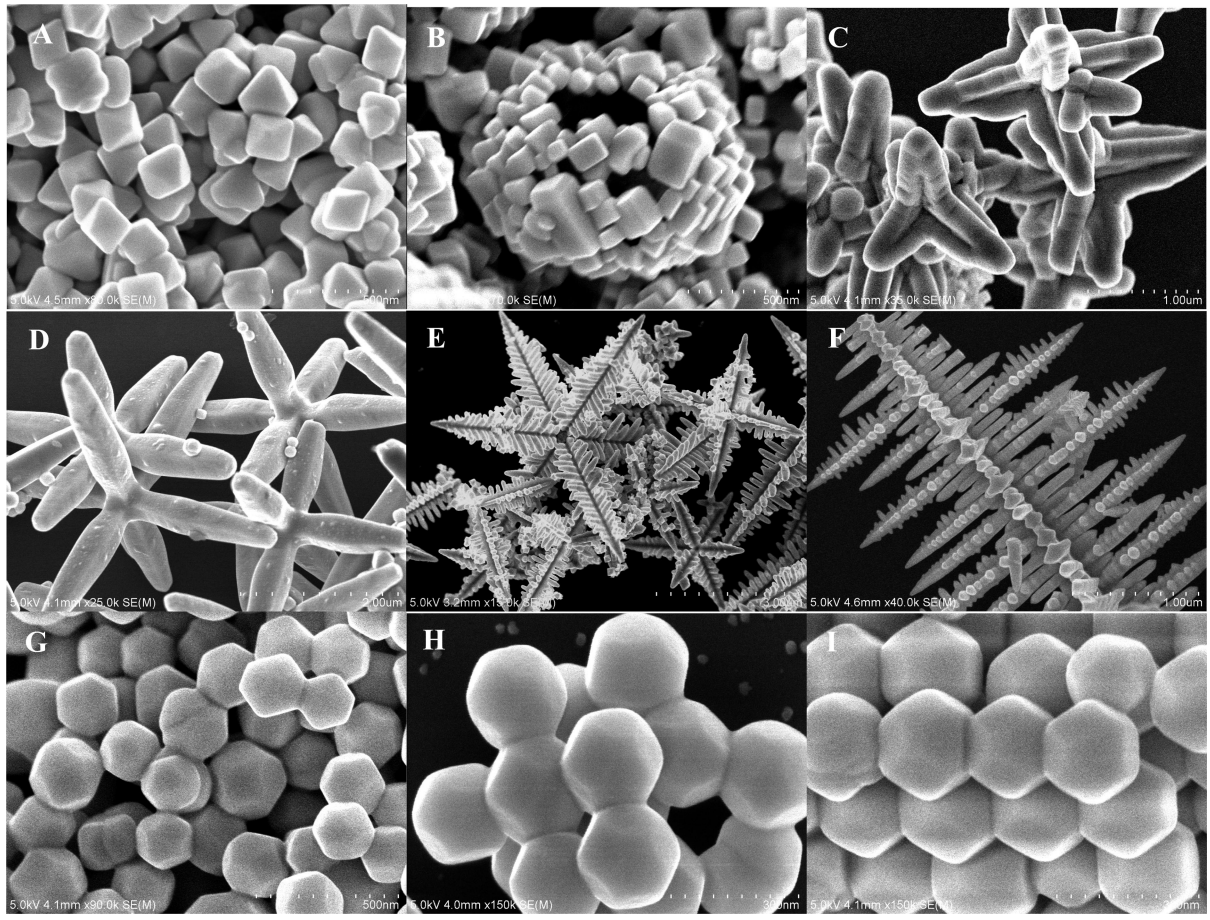

Figure 5. SEM images of PbS particles obtained under different conditions: (A) molar ratio S:Pb$(CH_3COO)_2 \cdot 5H_2O$, 1, octahedron; (B) molar ratio S:Pb$(CH3COO)_2 \cdot 5H_2O$, 2 and [CTAB]/4, truncated cubes; (C) reaction time elongated to 24 h, hexapod with pyramid arms; (D) double both the quantity of CTAB and reaction time, hexapods with smooth arms; (E) half of the original thiourea (starlike dendrites); (F) one-fourth of the original thiourea, dendrites. Different stages of the morphology evolution process of the as-assembled nanopattern: (G) dispersed PbS truncated octahedrons before assembly; (H−I) truncated octahedrons that tended to assembled together by sharing their {100} facets.

face area. The sharing of the {100} facets is because of which one has higher energy than that of {111} (Figure 5, panels G and E). In addition, dipolar interactions seem to be the most probable candidate for the driving force directing PbS nanocrystals to assemble into such multidimensional nanopatterns with specially high orientation (Figure 2, panels A and B, and Figure 5, panel F). As illustrated before, {111} facets are polar and their arrangement will determine the distribution of electric charge within the PbS nanocrystal. According to Murry's work,[43] a high fraction of PbS nanocrystals may also be with permanent dipole moments. The highest probability and the largest magnitude of the dipole moment are predicted along the [100] direction. The nanocrystals are driven to attach to the end of growing patterns when they have the largest dipole moment along the [100] axis. In the process reported here, the role of the hydrothermal treatment is on the one hand related to a continuous supply of the energy needed for production and assembly of the PbS crystals and on the other hand to a most uniform approach of supplying ions to all faces of octahedron crystal nuclei, so that the growth takes place on each face simultaneously. Surely only those nanocrystals which are with highly perfect uniformity have the potential for orderly self-assembly. Evidence for this has been found from the fact that the octahedral geometry is characteristic of most of the particles from similar conditions of the reaction though presented with a random sequence. Thus, here such a growth mechanism for the nanopattern may be plausible: when the thiourea was decomposed, numerous fcc PbS nuclei were formed, then preferential growth along the ⟨100⟩ and ⟨111⟩ directions leads to the formation of various PbS nanostructures. The nanopatterns were formed by assembling truncated octahedrons by sharing their {100} facets. Then, these patterns can be elongated through connecting other particles from the end of the matrix. The reaction environment promotes the surface domains on neighboring nanoparticles to match up by sharing one square face during the refluxing process, as reported previously; here the metastable nanostructure of truncated octahedron assembled into regular patterns to increase the portion of lower-index planes and satisfy

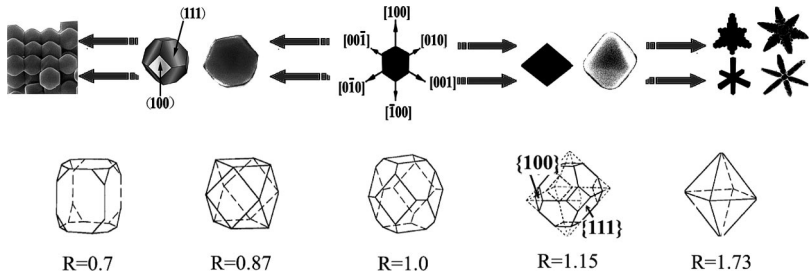

Figure 6. Schematic illustration of a proposed mechanism for the formation of the nanocrystals and the as-assembled nanopatterns. First, the fcc PbS nuclei are formed, then preferential growth along the ⟨100⟩ and ⟨111⟩ directions leads to the formation of various PbS nanostructures. The nanopatterns were formed by assembling truncated octahedrons by sharing their {100} facets. (b) Evolution in shapes of a series of {111}-based nanoparticles as the ratio of {111} to {100} increases.

both the rule of dipole interactions and the geometric criterion of a low energy.[36–43] On the basis of the above-mentioned orientation-dependent crystallinity and morphology evolution, a schematic illustration of the proposed particle growth and attachment mechanism responsible for the formation of the nanopatterns is listed in Figure 6.

CONCLUSIONS

In summary, large-scale synthesis of nanopatterns of well-defined truncated octahedron with highly geometrical symmetry and other superstructures of lead sulfide by a one-pot wet chemical reaction in pure water is possible. Each of these truncated octahedrons is apparently constructed by sharing the 24 edges in a mecon way. The results demonstrate that the branching growth process in solution can be precisely manipulated for the controlled growth of amazingly uniform crystalline structures with high geometrical symmetry, which is reflected in the primary crystal symmetry. This kind of nanopattern of truncated octahedron crystals with its 14 well-defined symmetries could find potential applications because of their unique structure such as a nanometer-sized construction element or a new kind of potential optical device that is independent or coupled with other materials. Moreover, we have also investigated the optical properties of the as-grown PbS polyhedron nanopatterns, indicating that our product is sensitive to the laser and can be photodegraded at much lower laser power thus conveniently converted to other environmental friendly materials. A corresponding mechanism of the formation of nanopatterns is tentatively suggested. These high-quality single crystalline PbS polyhedrons represent a new platform for further studies of nanoscale phenomena as well as for applications in various fields of nanotechnology.

EXPERIMENTAL SECTION

Synthesis of PbS Nanopatterns. In a typical reaction, 40 mL of 8 mol L^{-1} thiourea−H_2O is slowly added to 40 mL of 2 mol L^{-1} lead acetate ($Pb(Ac)_2 \cdot 4H_2O$, Aldrich) and CTAB (cetyltrimethylammonium bromine) dissolved in H_2O at room temperature. The resulting mixture is then transferred to a 150 mL autoclave and maintained at 150 °C for 24 h. The particles are precipitated after cooling the reaction mixture to room temperature and are separated and cleaned by repeated centrifugation with ethanol. The powder samples are thus used without any further size selection.

Characterization. The X-ray powder diffraction pattern of the as-prepared products was collected by a Rigaku X-ray diffractometer (Rigaku goniometer PMG-A2, CN2155D2, wavelength 0.15147 nm) with Cu Kα radiation. Transmission electron microscopy and scanning electron microscopy images were obtained by employing a JEOL JEM-2100F transmission electron microscopy and a Hitachi S4800 cold field emission scanning electron microscope. Raman spectra of the samples were collected using a LabRAM HR800 (HORIBA Jobin Yvon) confocal Raman spectrometer.

Acknowledgment. This project was financially supported by National Natural Science Foundation of China (50725208) and the Program for New Century Excellent Talents in University (NCET-04-0164) as well as by the State Key Project of Fundamental Research for Nanoscience and Nanotechnology (2006CB932300). S.Y. acknowledges the support from the Research Grants Council of Hong Kong (604206).

REFERENCES AND NOTES

1. Peng, X. G.; Manna, L.; Yang, W. D.; Wickham, J.; Scher, E.; Kadavanich, A.; Alivisators, A. P. Shape Control of CdSe Nanocrystals. *Nature* **2000**, *404*, 59–61.
2. Machol, J. L.; Wise, F. M.; Patel, R. C.; Tanner, D. B. Vibronic Quantum Beats in PbS Microcrystalites. *Phys. Rev. B* **1993**, *48*, 2819–2822.
3. Kane, R. S.; Cohen, R. E.; Silbey, R. Theoretical Study of the Electronic Structure of PbS Nanoclusters. *J. Phys. Chem.* **1996**, *100*, 7928–7932.
4. Zhou, G. J.; Lu, M. K.; Xiu, Z. L.; Wang, S. F.; Zhang, H. P.; Zhou, Y. Y.; Wang, S. M. Controlled Synthesis of High-Quality PbS Star-Shaped Dendrites, Multipods, Truncated Nanocubes, and Nanocubes and Their Shape Evolution Process. *J. Phys. Chem. B* **2006**, *110*, 6543–6548.
5. Trindade, T.; O'Brien, P.; Zhang, X. M.; Motevalli, M. Synthesis of PbS Nanocrystallites Using a Novel Single Molecule Precursors Approach: X-ray Single-Crystal Structure of $Pb(S_2CNEtPri)_2$. *J. Mater. Chem.* **1997**, *7*, 1011–1016.
6. Wang, S.; Yang, S. Preparation and Characterization of Oriented PbS Crystalline Nanorods in Polymer Films. *Langmuir* **2000**, *16*, 389–397.
7. Yu, D.; Wang, D.; Meng, Z.; Lu, J.; Qian, Y. Synthesis of Closed PbS Nanowires with Regular Geometric Morphologies. *J. Mater. Chem.* **2002**, *12*, 403–405.
8. Yu, D.; Wang, D.; Zhang, S.; Liu, X.; Qian, Y. Multi-Morphology PbS: Frame—Film Structures, Twin Nanorods, and Single-Crystal Films Prepared by a Polymer-Assisted Solvothermal Method. *J. Cryst. Growth* **2003**, *249*, 195–200.

9. Lee, S. M.; Jun, W. W.; Cho, S. N.; Cheon, J. Single-Crystalline Star-Shaped Nanocrystalsand Their Evolution: Programming the Geometry of Nano-Building Blocks. *J. Am. Chem. Soc.* **2002**, *124*, 11244–11245.
10. Ma, Y.; Qi, L.; Ma, J.; Cheng, H. Hierarchical, Star-Shaped PbS Crystals Formed by a Simple Solution Route. *Cryst. Growth Des.* **2004**, *4*, 351–354.
11. Ni, Y.; Liu, H.; Wang, F.; Liang, Y.; Hong, J.; Ma, X.; Xu, Z. Shape Controllable Preparation of PbS Crystals by a Simple Aqueous Phase Route. *Cryst. Growth. Des.* **2004**, *4*, 759–764.
12. Yan, H.; He, R.; Johnson, J.; Law, M.; Saykally, R. J.; Yang, P. Dendritic Nanowire Ultraviolet Laser Array. *J. Am. Chem. Soc.* **2003**, *125*, 4728–4729.
13. Lu, Q.; Gao, F.; Komarneni, S. Biomolecule-Assisted Synthesis of Highly Ordered Snowflakelike Structures of Bismuth Sulfide Nanorods. *J. Am. Chem. Soc.* **2004**, *126*, 54–55.
14. Zhang, J. X.; Qiu, L. Y.; Jin, Y. Controlled Nanoparticles Formation by Self-assembly of Novel Amphiphilic Polyphosphazenes with Poly(N-isopropylacrylamide) and Ethyl Glycinate as Side Groups. *React. Funct. Polym.* **2006**, *66*, 1630–1640.
15. Long, D. L.; Burkholder, E.; Cronin, L. Polyoxometalate Clusters, Nanostructures and Materials: From Self Assembly to Designer Materials and Devices. *Chem. Soc. Rev.* **2007**, *36*, 105–121.
16. Bartlett, P. N.; Birkin, P. N.; Ghanem, M. A.; de Groot, P.; Sawicki, M. The Electrochemical Deposition of Nanostructured Cobalt Films from Lyotropic Liquid Crystalline Media. *J. Electrochem. Soc.* **2001**, *148*, C119–C123.
17. Hulteen, J. C.; Martin, C. R. A General Template-Based Method for the Preparation of Nanomaterials. *J. Mater. Chem.* **1997**, *7*, 1075–1087.
18. Thurn-Albrecht, T.; Schotter, J.; Kästle, G. A.; Emley, N.; Shibauchi, T.; Krusin-Elbaum, L.; Guarini, K.; Black, C. T.; Tuominen, M. T.; Russell, T. P. Ultrahigh-Density Nanowire Arrays Grown in Self-Assembled Diblock Copolymer Templates. *Science* **2000**, *290*, 2126–2129.
19. Bartlett, P. N.; Birkin, P. R.; Ghanem, M. A. Electrochemical Deposition of Macroporous Platinum. Palladium and Cobalt Films Using Polystyrene Latex Sphere Templates. *Chem. Commun.* **2000**, 1671–1672.
20. Xu, L.; Zhou, W. L.; Frommen, C. R.; Baughman, H.; Zakhidov, A. A.; Malkinski, L.; Wang, J. Q.; Wiley, J. B. Electrodeposited Nickel and Gold Nanoscale Metal Meshes with Potentially Interesting Photonic Properties. *Chem. Commun.* **2000**, 997–998.
21. Corres, J. M.; Villar, I.; Matias, I. R. Fiber-Optic pH-Sensors in Long-Period Fiber Gratings Using Electrostatic Self-Assembly. *Opt. Lett.* **2007**, *32*, 29–31.
22. Peng, Z. A.; Peng, X. Mechanisms of the Shape Evolution of CdSe Nanocrystals. *J. Am. Chem. Soc.* **2001**, *123*, 1389–1398.
23. Alivisatos, A. P. Perspectives on the Physical Chemistry of Semiconductor Nanocrystals. *J. Phys. Chem.* **1996**, *100*, 13226–13239.
24. Wu, C.; Yu, S.; Antonietti, M. Complex Concaved Cuboctahedrons of Copper Sulfide Crystals with Highly Geometrical Symmetry Created by a Solution Process. *Chem. Mater.* **2006**, *18*, 3599–3601.
25. Krauss, T. D.; Wise, F. W.; Tanner, D. B. Observation of Coupled Vibrational Modes of a Semiconductor Nanocrystal. *Phys. Rev. Lett.* **1996**, *76*, 1376–1379.
26. Nanda, K. K.; Sahu, S. N.; Soni, R. K.; Tripathy, S. Raman Spectroscopy of PbS Nanocrystalline Semiconductors. *Phys. Rev. B* **1998**, *58*, 15405–15407.
27. Batonneau, Y.; Bremard, C.; Merli, C. Microscopic and Imaging Raman Scattering Study of PbS and Its Photo-Oxidation Products. *J. Raman Spectrosc.* **2000**, *31*, 1113–1119.
28. Ming, W.; Liu, X.; Yu, W.; Qian, Y. Dendritic Growth of PbS Crystals with Different Morphologies. *J. Cryst. Growth* **2003**, *257*, 384–389.
29. Kuang, D. A.; Xu, Fang, Y.; Liu, H.; Frommen, C.; Fenske, D. Surfactant-Assisted Growth of Novel PbS Dendritic Nanostructures via Facile Hydrothermal Process. *Adv. Mater.* **2003**, *15*, 1747–1750.
30. Ilic, B.; Neuzil, P.; Stanczyk, T. Observation of Dendritic Growth with Colloidal Au Particles. *J. Mater. Sci. Lett.* **2000**, *19*, 193–195.
31. Zhao, N.; Qi, L. Low-Temperature Synthesis of Star-Shaped PbS Nanocrystals in Aqueous Solutions of Mixed Cationic/Anionic Surfactants. *Adv. Mater.* **2006**, *18*, 359–362.
32. Wang, Z. L. Transmission Electron Microscopy of Shape-Controlled Nanocrystals and Their Assemblies. *J. Phys. Chem. B* **2000**, *104*, 1153–1175.
33. Russell, G.; Henrichs, P.; Hewitt, J.; Grashof, H.; Sandhu, M. Monomer Sequence Distributions in Four-Component Polyesters as Determined By Carbon-13 and Hydrogen-1 NMR. *Macromolecules* **1981**, *14*, 1764–1770.
34. Barroso-Bujans, F.; Martinez, R.; Ortiz, P. Structural Characterization of Oligomers from The Polycondensation of Citric Acid with Ethylene Glycol and Long-Chain Aliphatic Alcohols. *J. Appl. Polym. Sci.* **2003**, *88*, 302–306.
35. Wang, Y. L.; Jiang, X. C.; Xia, Y. N. A Solution-Phase, Precursor Route to Polycrystalline SnO_2 Nanowires That Can Be Used for Gas Sensing under Ambient Conditions. *J. Am. Chem. Soc.* **2003**, *125*, 16176–16177.
36. Tang, Z.; Kotov, N. A.; Giersig, M. Spontaneous Organization of Single CdTe Nanoparticles into Luminescent Nanowires. *Science* **2002**, *297*, 237–240.
37. Pacholski, C.; Kornowski, A.; Weller, H. Self-Assembly of ZnO: From Nanodots to Nanorods. *Angew. Chem., Int. Ed.* **2002**, *41*, 1188–1191.
38. Korgel, B. A.; Fitzmaurice, D. Self-Assembly of Silver Nanocrystals into Two-Dimensional Nanowire Arrays. *Adv. Mater.* **1998**, *10*, 661–665.
39. Lu, W.; Gao, P.; Jian, W. B.; Wang, Z. L.; Fang, J. Perfect Orientation Ordered in-Situ One-Dimensional Self-Assembly of Mn-Doped PbSe Nanocrystals. *J. Am. Chem. Soc.* **2004**, *126*, 14816–14821.
40. Tang, Z. Y.; Zhang, Z. L.; Wang, Y.; Glotzer, S. C.; Kotov, N. A. Self-Assembly of CdTe Nanocrystals into Free-Floating Sheets. *Science* **2006**, *314*, 274–278.
41. Harfenist, S. A.; Wang, Z. L.; Alvarez, M. M.; Vezmar, I.; Whetten, R. L. Three-dimensional Hexagonal Close-packed Superlattice of Passivated Ag Nanocrystals. *Adv. Mater.* **1997**, *9*, 817–822.
42. Wang, Z. L. Structural Analysis of Self-Assembling Nanocrystal Superlattices. *Adv. Mater.* **1998**, *10*, 13–30.
43. Cho, K. S.; Talapin, D. V.; Gaschler, W.; Murray, C. B. Designing PbSe Nanowires and Nanorings through Oriented Attachment of Nanoparticles. *J. Am. Chem. Soc.* **2005**, *127*, 7140–7147.